High-Resolution 3D MR Neurography of the Wrist using Phase-Cycling Diffusion-Sensitized Driven-Equilibrium (pcDSDE)

Masami Yoneyama[1], Makoto Obara[1], Yuriko Ozawa[2], Hajime Tanji[3], Masanobu Nakamura[1], Tomoyuki Okuaki[1], Takashi Tabuchi[2], Satoshi Tatsuno[2], Ryuji Sashi[2], and Marc Van Cauteren[1]

[1]*Philips Electronics Japan, Tokyo, Japan,* [2]*Yaesu Clinic, Tokyo, Japan,* [3]*Imaging Center, Kita-Fukushima Medical Center, Fukushima, Japan*

TARGET AUDIENCE: Researchers and clinicians interested in MR neurography and peripheral nerve diseases.

PURPOSE: Carpal tunnel syndrome (CTS) is a median entrapment neuropathy that causes various symptoms due to median nerve compression at the wrist in the carpal tunnel[1-4]. The role of MRI in diagnosis of CTS is depiction of the anatomical detail of peripheral nerves and the pathological changes related to entrapment[2]. Recently, a new method[5] based on motion-sensitized driven-equilibrium (MSDE) prepared 3D turbo spin-echo has been emerged for high-resolution 3D MR neurography. Although this sequence can provide excellent quality images in the brachial plexus, lumbosacral plexus and intracranial nerves, it occasionally yields poor image quality in the extremities due to weak contrast between nerves and surrounding tissues because MSDE provides only "low b-value" effect. On the other hand, so-called diffusion-sensitized driven equilibrium (DSDE[6]), a variant of MSDE, has been developed. DSDE is an optimized pre-pulse for enabling higher b-value and has been applied for distortion-free DWI[7-9] and motion-insensitive MR neurography in the brachial plexuss[6]. In this study, we attempted to use DSDE technique for achieving high-resolution MR neurography in the wrist.

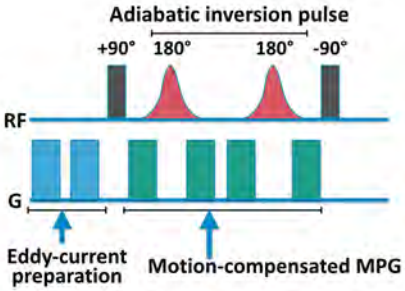

Figure 1. Scheme of DSDE preparation pulse. The DSDE pulse has three important features (adiabatic pulse, eddy-current prep and motion-compensated MPG) for enabling high b-value.

METHODS: Scheme of DSDE pre-pulse is shown in **Fig.1**. DSDE pulse has three important features for enabling higher b-value. Adiabatic refocusing pulses and additional gradients inserted in front of the pre-pulse (eddy-current prep[10]) were applied to reduce B_0 and B_1 inhomogeneity, and eddy-current artifacts. Motion-compensated motion probing gradients (unipolar MPGs) are used not only for reducing motion effect but also for stabilizing the image quality in higher b-value[6].

Because of the diffusion anisotropy of the human nervous system, peripheral nerves are best visualized when applying MPGs perpendicular to the course of the nerves, while nerves are not well visualized when applying MPGs parallel to the course of the nerves[11,12]. In this study, two directions of strong MPGs were placed in both the anterior-posterior and right-left directions, which are most perpendicular to the trajectories of the nerves in the wrist. However, to suppress the vessel signals (veins) that flow in the same direction as the nerves, we added a weak MPG parallel to the course of the nerves (superior-inferior direction). Thus, we adopted the asymmetric MPGs in three axes.

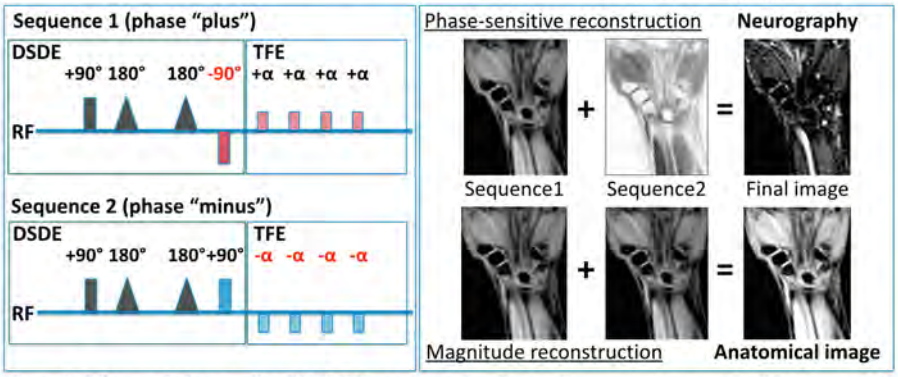

Figure 2. Scheme of phase-cycling DSDE-TFE sequence. Two types of sequences are acquired. In sequence1 and 2, phases of RF are opposite at the flip-back pulse of the DSDE and TFE sequence. As a result, neurography images are obtained by addition of respective phase-sensitive images and anatomical (proton-density weighted) images are obtained by addition of both magnitude-images from same-data.

To eliminate the T1-effects, which are given by readout-sequence (T1-turbo field echo: T1TFE) and deteriorate diffusion weighted contrast, phase-cycling scheme is applied[13,14]. Scheme of phase-cycling DSDE-TFE sequence is shown in **Fig.2**. This method always requires the acquisition of two types of sequences (sequence1 and 2). In sequence1 and 2, phases of RF pulse are opposite at the flip-back pulse of DSDE pulse and TFE sequence. As a result, neurography images are obtained by addition of respective phase-sensitive images, and anatomical (proton-density weighted) images are obtained by addition of both magnitude-images from the identical data.

A total of six volunteers were examined with 3.0T whole-body clinical system (Achieva TX, Philips Healthcare). The study was approved by the local IRB, and written informed consent was obtained from all subjects. Imaging parameters were; Coronal, voxel size=1.44mm^3, b-value=1100s/mm^2, DSDE preparation time (prep-time)=110ms, gradient strength phase/freq/slice=25/5/25mT/m, shot interval=3000ms, flip angle=8°, turbo factor=30, ProSet 1331, and total acquisition time=7m30s.

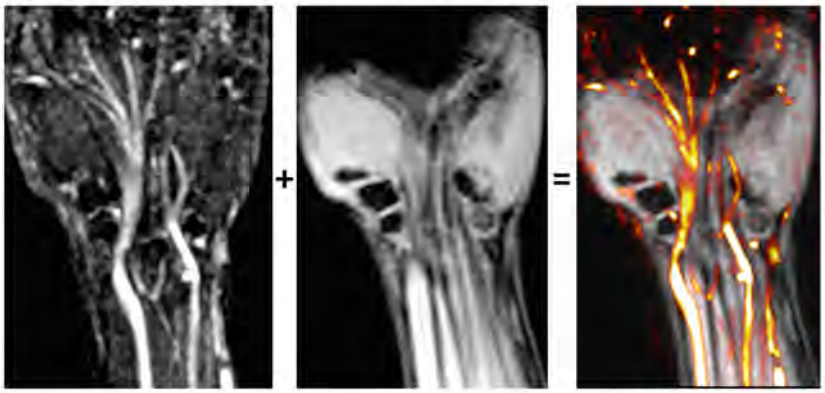

Figure 3. Representative images of MR neurography of the wrist by using pcDSDE-TFE sequence. Furthermore, pcDSDE sequence could provide "self-fusion" images simultaneously by two types of reconstructed images (neurography images and anatomical images)

RESULTS and DISCUSSION: Representative images of MR neurography of the wrist, by using pcDSDE-TFE sequence, are shown in **Fig.3**. pcDSDE-TFE clearly shows both anatomies and courses of median nerve, ulnar nerve and their branches on the MIP images. This sequence could provide high-quality images with sufficient SNR despite the use of long prep-time (110ms) and high b-value (1100s/mm^2). Furthermore, pcDSDE could simultaneously offer "self-fusion" images by using two types of reconstructed images (neurography images and anatomical images). Self-fusion images may help the diagnosis of CTS by giving further detailed anatomic relation.

CONCLUSION: This study showed a new scheme for MR neurography of the wrist by using phase-cycled DSDE-TFE sequence. This sequence has great potential to stably depict peripheral nerves in the extremities. Further clinical investigation is needed.

REFERENCES: [1]Uchiyama, J Orthop Sci 2010;15:1–13; [2]Miller, AJR 2010;195:585-94; [3]Khalil, Eur Radiol 2008;18:2283–2291; [4]Cha, J Magn Reson Imaging 2014;4:789–795; [5]Yoneyama, Magn Reson Med Sci 2013;12:111–119; [6]Obara, Proc. ISMRM 2011:4023; [7]Yamashita, Eur J Radiol. 2013;82:e471-5; [8]Hiwatashi, AJNR 2014;35:95-8; [9]Schakel, Proc. ISMRM 2014:0668; [10]Obara, J Magn Reson Imaging 2014;4:824-831; [11]Takahara, Eur Radiol 2009; 20:1221–1226; [12]Takahara, Neuroradiology 2011; 53:109–116; [13]Coremans, J Magn Reson 1997;124:323–42; [14]Thomas, Magn Reson Med 1998;39:950–60.48:739–743 (2002).